

AD-A121 983

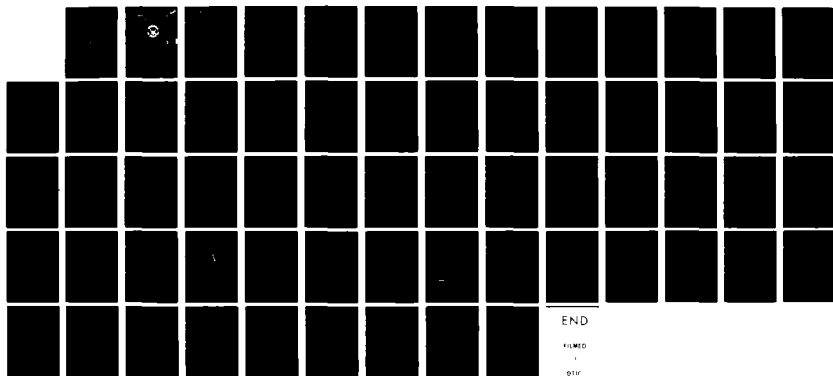
TWO-PHASE LAMINAR BOUNDARY LAYER FLOW AROUND A WEDGE
(U) NAVAL POSTGRADUATE SCHOOL MONTEREY CA D V DORD
JUN 82

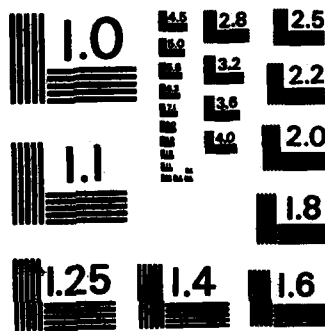
1/1

UNCLASSIFIED

F/G 28/4

NL





MICROCOPY RESOLUTION TEST CHART
NATIONAL BUREAU OF STANDARDS-1963-A

AD A121983

NAVAL POSTGRADUATE SCHOOL
Monterey, California



THESIS

DTIC
ELECTE
NOV 30 1982
S D

TWO-PHASE LAMINAR BOUNDARY LAYER
FLOW AROUND A WEDGE

by

Dirk van Dord

June 1982

Thesis Advisor:

James V. Sanders

Approved for public release; distribution unlimited

DTIC FILE COPY

88 11 30 06

UNCLASSIFIED

SECURITY CLASSIFICATION OF THIS PAGE (When Data Entered)

REPORT DOCUMENTATION PAGE		READ INSTRUCTIONS BEFORE COMPLETING FORM
1. REPORT NUMBER	2. GOVT ACCESSION NO.	3. RECIPIENT'S CATALOG NUMBER
	AD-A212983	
4. TITLE (and Subtitle)		5. TYPE OF REPORT & PERIOD COVERED
Two-Phase Laminar Boundary Layer Flow Around a Wedge		Master's Thesis June 1982
7. AUTHOR(s)		6. PERFORMING ORG. REPORT NUMBER
Dirk van Dord		
8. PERFORMING ORGANIZATION NAME AND ADDRESS		9. CONTRACT OR GRANT NUMBER(s)
Naval Postgraduate School Monterey, California 93940		
11. CONTROLLING OFFICE NAME AND ADDRESS		10. PROGRAM ELEMENT, PROJECT, TASK AREA & WORK UNIT NUMBERS
Naval Postgraduate School Monterey, California 93940		
12. REPORT DATE		13. NUMBER OF PAGES
June 1982		62
14. MONITORING AGENCY NAME & ADDRESS (if different from Controlling Office)		15. SECURITY CLASS. (of this report)
		Unclassified
		15a. DECLASSIFICATION/DOWNGRADING SCHEDULE
16. DISTRIBUTION STATEMENT (of this Report)		
Approved for public release; distribution unlimited		
17. DISTRIBUTION STATEMENT (of the abstract entered in Block 20, if different from Report)		
18. SUPPLEMENTARY NOTES		
19. KEY WORDS (Continue on reverse side if necessary and identify by block number)		
Laminar Flow Wedge Flow Two-Phase Flow Drag Reduction Boundary Layer Blowing		
20. ABSTRACT (Continue on reverse side if necessary and identify by block number)		
<p>This thesis theoretically presents the phenomena involved in the flow of an incompressible fluid over a wedge with a second incompressible, lighter, and less viscous fluid blown through the surface of the wedge. A method is developed to determine the inner fluid layer thickness, the wall shear stress and the resulting local drag reduction. The results predict substantial drag reduction.</p>		

DD FORM 1473

JAN 73

EDITION OF 1 NOV 65 IS OBSOLETE
S/N 0102-014-6001

UNCLASSIFIED

SECURITY CLASSIFICATION OF THIS PAGE (When Data Entered)

Approved for public release; distribution unlimited

Two-Phase Laminar Boundary Layer Flow
Around a Wedge

by

Dirk van Dord
Lieutenant Commander, Royal Netherlands Navy

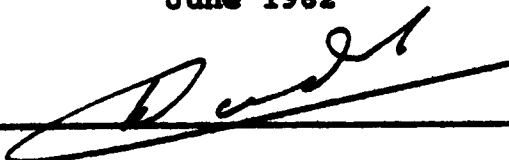
Submitted in partial fulfillment of the
requirements for the degree of

MASTER OF SCIENCE IN ENGINEERING ACOUSTICS

from the

NAVAL POSTGRADUATE SCHOOL
June 1982

Author:



Approved by:


Thesis Advisor


Second Reader


Chairman, Engineering Acoustics Academic
Committee


Dean of Science and Engineering

Accession For	
NTIS GRA&I	<input checked="" type="checkbox"/>
DTIC TAB	<input type="checkbox"/>
Unannounced	<input type="checkbox"/>
Justification	
By	
Distribution/	
Availability Codes	
Dist	Avail and/or Special
A	



ABSTRACT

This thesis theoretically presents the phenomena involved in the flow of an incompressible fluid over a wedge with a second incompressible, lighter, and less viscous fluid blown through the surface of the wedge. A method is developed to determine the inner fluid layer thickness, the wall shear stress and the resulting local drag reduction. The results predict substantial drag reduction.

TABLE OF CONTENTS

I.	INTRODUCTION	10
II.	BACKGROUND	11
	A. DISCUSSION OF RELATED PAPERS	11
	1. J. Pretsch	11
	2. E. J. Watson	12
	3. R. D. Cess and E. M. Sparrow	13
	4. K. Nickel	15
	5. R. D. Cess and E. M. Sparrow	15
	6. E. M. Sparrow, V. K. Jonsson and E. R. G. Eckert	15
	7. H. P. Eichenberger and J. D. Offutt	16
	8. W. S. Bradfield, R. O. Barkdoll and J. T. Byrne	17
	9. T. J. Lang	18
	10. E. R. van Driest	18
	B. QUO VADIS	19
III.	THEORY	20
	A. GOVERNING EQUATIONS	20
	B. TRANSFORMED EQUATIONS	22
IV.	EXPLORED WAYS OF SOLUTION	27
	A. SERIES SOLUTION	27
	B. NUMERICAL SOLUTIONS	28
	1. IODE	28

2. Desk Top Computer	30
V. SOLUTIONS	31
A. DEFINITION OF THE PROBLEM	31
B. TESTING THE PROGRAM	33
1. Number of Steps of Independent Variable	33
2. One Fluid Flow	33
3. Solution for R Close to 1	33
4. Solution for Small Wedge Angles	33
VI. RESULTS	34
A. DEFINITION OF A SAMPLE PROBLEM	34
B. THICKNESS OF THE INNER FLUID LAYER	34
C. WALL SHEAR STRESS	35
D. VELOCITY PROFILES	35
E. DRAG REDUCTION	36
F. REQUIRED POWER	37
VII. CONCLUSIONS AND RECOMMENDATIONS	39
APPENDIX A. "BASIC" PROGRAM FOR WANG DESK TOP COMPUTER TO SOLVE TWO FLUID LAMINAR FLOW CHARACTERISTICS	40
APPENDIX B. FIGURES	43
APPENDIX C. TABLES	50
LIST OF REFERENCES	59
INITIAL DISTRIBUTION LIST	61

LIST OF SYMBOLS

C	constant
E_T	internal energy
$f_g(\eta_g)$	dimensionless stream function inner-fluid
$f_L(\eta_L)$	dimensionless stream function outer-fluid
$g(x)$	scale factor for y
K	integration constant
L	reference length
m	constant defined by $\frac{\beta}{2-\beta}$
\dot{m}	mass flow rate
P	local pressure
PR	Prandtl number
P_{STAG}	stagnation pressure
Q	heat into the system
R	fluid properties ratio defined by $R = \left\{ \frac{(\rho u)_L}{(\rho u)_g} \right\}^{\frac{1}{2}}$
Re	Reynolds number
R_g	gas constant
T	local temperature
T_w	wall temperature
T_∞	temperature in the free stream
u	velocity component tangential to surface
$U(x)$	potential speed
U_∞	reference speed

v	velocity component normal to surface
v_w	blowing velocity at the wall
w	velocity component normal to u and v
\vec{w}	velocity
W	work done by the system
x	arc length along the surface
X	body force in x -direction
y	direction normal to surface
y_1	dummy variable for f
y_2	dummy variable for f'
y_3	dummy variable for f''
Y	body force in y -direction
z	direction normal to x and y
Z	body force in z -direction
α	similarity constant given by $\frac{L}{U_\infty} \frac{g(x)}{dx} (U(x)g(x))$
β	"dimensionless" wedge angle (angle is $\beta\pi$)
$\delta(x)$	boundary layer thickness
η	dimensionless similarity variable
η_{gi}	dimensionless inner fluid layer thickness
ξ	dimensionless parameter
ρ	mass density
μ	dynamic viscosity
ν	kinematic viscosity
ψ	stream function
τ	shear stress

τ_w

shear stress at the wall

τ_0

reference shear stress

ACKNOWLEDGMENT

The author expresses his appreciation to Dr. J. V. Sanders for leading him through the darkness of scientific research and for his availability to assist in breaking deadlocks, and to Dr. F. J. Jouaillec who, by his fresh ideas in these trying times, was able to give impulses to the progress.

Special thanks are given to my wife Carla van Dord-Zeegers and our three sons Bas, Lex and Rob for their patience and endurance.

I. INTRODUCTION

The ever increasing operating depths and speeds of modern submarines and the much higher resistance to the effects of contact or nearby underwater explosions all require a dramatic increase in the speed of underwater weapons. The existing power plant systems seem to have reached their limits in power density and radical changes in body shapes are limited by launching facilities. The answer might lie in the field of boundary layer control. Possibilities are injection of polymers into the boundary layer to maintain laminar flow, suction to remove potential turbulence, more sophisticated weapon shapes to reduce form drag, or introducing a gas layer between the surface of the body and the liquid.

Of all the options, the two-phase boundary layer seems to be the most promising possibility for obtaining an order of magnitude increase in speed.

In this thesis, a method is developed to calculate the properties of the laminar, two-phase flow produced by injecting a light, incompressible low-viscosity fluid into the boundary layer of the incompressible flow over a wedge. This is just a step on the long way to a high speed underwater weapon.

II. BACKGROUND

A. DISCUSSION OF RELATED PAPERS

An extensive literature search was carried out and the relevant papers are discussed below. The reduction of drag by use of polymers is deleted from this survey because the drag reduction expected by this method is probably not sufficient to increase the maximum speed of the underwater vehicle substantially. Amazingly enough, the most recent paper in the field of two-fluid laminar boundary layer flow was published back in 1969.

1. J. Pretsch [1]

Pretsch starts with Prandtl's boundary layer equations for single-phase flow with suction or blowing:

$$u \frac{\partial u}{\partial x} + v \frac{\partial u}{\partial y} = U \frac{\partial U}{\partial x} + \nu \frac{\partial^2 u}{\partial y^2}$$

and boundary conditions $y = 0 : u = 0, v = v_w; y/\sqrt{Re} \rightarrow \infty : u = 0$ where u is the velocity tangential to the surface, v is the velocity normal to the surface, x is the arc length along the surface, y is the normal to the surface, $U(x)$ is the potential velocity, ν is kinematic viscosity, $v_w(x)$ is the normal velocity or blowing velocity at the surface and Re is the Reynolds number, $Re = \frac{Ux}{\nu}$.

For strong suction ($v_0 \rightarrow -\infty$) the above equations simplify to a second order, ordinary differential equation of the form

$$\frac{d^2 u}{d\xi^2} + \frac{du}{d\xi} = 0 \quad \text{where } \xi = -\frac{y v_w}{v}$$

and boundary conditions $\xi = 0 : u = 0$

$\xi \rightarrow \infty : u = U(x)$

The solution of this equation is the velocity profile

$$\frac{u}{U(x)} = 1 - e^{-\xi}$$

For strong blowing ($v_w \rightarrow \infty$) the assumption is made that the viscosity term can be neglected and the above equations again simplify to a second order, ordinary differential equation but now nonlinear.

For a number of values for similarity parameters, Pretsch gives analytical expressions for solutions of flat plate and wedge flow.

The assumption of negligible viscosity is too restrictive for the case under investigation in this thesis.

2. E. J. Watson [2]

This extensive report consists of three parts, i.e. Theory of Similar Velocity Distributions, Flow with Uniform Suction, and Flow with Variation of Suction Velocity. The report is based on the asymptotic theory of boundary layer

flow. Although the author is aware of the existence of Pretsch's work, no comparison of results is made.

In Part I the author arrives at a number of tables giving velocity distribution and coefficients of the series expansions as functions of similarity related constants and dimensionless parameters.

In Part II the similarity principle is abandoned but the suction velocity is uniform. The velocity is expanded into a series from which series for momentum and displacement thickness and skin friction are derived. In the subsequent section a number of applications are investigated and the results are totalized in a number of tables.

In Part III the asymptotic theory is extended to cover general two dimensional flow with arbitrary distributions of mainstream velocity and suction velocity. The results are again displayed in tables. The author also derives the results in Part I as a special case of Part III.

As this report only deals with suction it is not of direct interest to this study.

3. R. D. Cess and E. M. Sparrow [3]

This paper deals with a two-phase flow in forced convection over a flat plate. The inner fluid is obtained by boiling the outer fluid at the wall so that a vapor film is formed. The authors arrive at the following conservation equations:

$$f_g''' + f_g f_g'' = 0$$

$$\theta'' + PR f_g \theta' = 0 \quad \text{where } \theta = \frac{T - T_\infty}{T_w - T_\infty}$$

$$f_L''' + f_L f_L'' = 0$$

with boundary conditions:

plate surface: $f_g(0) = f_g'(0) = 0, \theta(0) = 1$

interface: $f_L(0) = \left(\frac{(\rho\mu)_g}{(\rho\mu)_L} \right)^{1/2} f_g(\eta_{gi})$

$$f_L'(0) = f_g'(\eta_{gi})$$

$$f_L''(0) = \left(\frac{(\rho\mu)_g}{(\rho\mu)_L} \right)^{1/2} f_g''(\eta_{gi})$$

$$\theta(\eta_\delta) = 0$$

free stream: $f_L'' \rightarrow 2$ as $\eta_L \rightarrow \infty$

where f_g and f_L are the stream functions for respectively inner and outer fluid, T is the local temperature, T_w is the temperature at the wall, T_∞ is the temperature in the free stream, PR is the Prandtl number, ρ is the mass density and μ is the dynamic viscosity. f_g is a function of the dimensionless parameter η_g defined by $\eta_g = \frac{y}{2} \sqrt{\frac{U_\infty}{\nu_g x}}$. η_{gi} is the value for this parameter at the interface of the two fluids. f_L is a function of the dimensionless parameter η_L defined by $\eta_L = \frac{y}{2} \sqrt{\frac{U_\infty}{\nu_L x}}$. The subscripts L and g refer to respectively outer and inner fluid. The primes denote differentiation with respect to the relevant dimensionless parameter. This

problem is solved by using an Emmons-Leigh [4] table and a successive approximation procedure.

4. K. Nickel [5]

In this paper, the laminar flow of an incompressible fluid without heat transfer is investigated using a method of bounding the solutions applied to Prandtl's equations. After introducing the well-known dimensionless parameters η and $f(\eta)$, Prandtl's partial differential equations reduce to the ordinary, third order non-linear differential equation:

$$f''' + ff'' + \beta(1 - f'^2) = 0$$

with boundary conditions: $f(0) = f_0$

$$f'(0) = 0$$

$$f'(\infty) = 1$$

The solutions are reflected in a number of graphs, especially "abbildung 8" giving $f''(0)$ as a function of β and f_0 will prove to be very useful in this thesis.

5. R. D. Cess and E. M. Sparrow [6]

This paper is an extension of the paper discussed in Section 3 above and deals with the case of a subcooled fluid. To extend the earlier results it was necessary to consider the conservation of energy within the fluid. The results are again reflected in a number of figures.

6. E. M. Sparrow, V. K. Jonsson and E. R. G. Eckert [7]

In this paper the laminar two-phase flow, obtained by injecting gas into a liquid at the wall of a flat plate, was

investigated. The authors arrive at the following ordinary differential equations

for the gas: $f_g''' + f_g f_g'' = 0$

for the liquid: $f_L''' + f_L f_L'' = 0$

with boundary conditions:

at the wall: $f_g(0) = f_{g0}$ (blowing parameter)

$f_g'(0) = 0$ (no slip condition)

at the interface: $f_g(\eta_{gi}) = f_L(0) = 0$ (no mass transfer)

$f_g''(\eta_{gi}) = R f_L''(0)$ (stress continuous)

$$\text{where } R = \left\{ \frac{(\rho\mu)_L}{(\rho\mu)_g} \right\}^{\frac{1}{2}}$$

$f_g'(\eta_{gi}) = f_L'(0)$ (velocity continuous)

for $\eta_L \rightarrow \infty$: $f_L'(\eta_L) \rightarrow 2$ (velocity approaches U_∞)

The authors solve these equations by applying a series expansion and subsequently a successive approximation procedure, similar to the one described in the paper by Cess and Sparrow (Section 3 above).

The results are given in a table and a graph. It is proven that evaporation at the interface only works advantageous.

7. H. P. Eichenberger and J. D. Offutt [8]

Under assumption of

- shear stress in liquid is negligible
- interfacial velocity and pressure distribution are those imposed by the potential flow

- the inertia of the gas is negligible
- the gas flow is laminar
- body moves steadily through water at zero incidence
- gas and water properties are constant; in particular the density of the gas remains constant

the problem of a two-phase flow over different kinds of bodies is solved by a finite differences method. Results are given in a number of graphs.

8. W. S. Bradfield, R. O. Barkdoll and J. T. Byrne [9]

This paper discusses experiments with a "gassing" model to investigate possible drag reductions. The vapor layers were obtained by film boiling, sublimation of a solid surface and chemical reactions. The experiments indicated that for film boiling a region exists for which a stable vapor layer may be expected.

Assuming

- steady, two dimensional laminar flow
- pressure everywhere constant
- heated surface temperature constant
- temperature of liquid vapor interface is equal to saturated liquid temperature
- thermodynamic and transport properties of liquid and vapor are constant
- thermal radiation effect on vapor and liquid layers is neglected
- buoyancy effect on forced convection boundary layers is neglected
- velocity and temperature profiles are linear in vapor and parabolic in liquid

and using the Pohlhausen integral method the results of the experiments are predicted. In some of the experiments dramatic instabilities were found, and the authors had to conclude that producing a stable vapor layer between a surface and a liquid drastically reduces friction drag but unstable, two-phase flow (like nucleate boiling and uncontrolled sublimation) may actually cause the drag to increase.

9. T. J. Lang [10]

In this patent Lang "designed" a torpedo capable of using the gas film drag reduction phenomena. The lift is provided by the body shape and the exhaust gases are used to produce the gas layer. At the rear end of the torpedo the gas layer is removed by suction.

10. E. R. van Driest [11]

The author indicates that the quest for higher speeds of underwater craft can be solved by using the knowledge acquired in high speed aerodynamics.

In a number of figures the author gives local friction coefficients as a function of Reynolds number, speed, wall temperature and ocean depth. Further effects of hydrodynamic heating, cavitation and insertion of additives are discussed.

The author concludes that although the propulsion systems have to be developed, it is, in principle, possible to obtain high velocities for underwater vehicles.

B. QUO VADIS

Considering the above discussion it was felt that more knowledge had to be obtained of the phenomena taking place in the two-phase boundary layer. A first step would be to extend the work on flat plates to two-dimensional bodies with pressure-gradients. It is logical to follow the paper of Sparrow, Jonsson and Eckert [7], discussed above in Section A-6.

III. THEORY

A. GOVERNING EQUATIONS

To predict the skin friction and drag characteristics from first principles the starting position is based on the basic conservation laws governing the velocity distribution, here in Cartesian coordinates,

Continuity:
$$\frac{\partial \rho}{\partial t} + \frac{\partial (\rho u)}{\partial x} + \frac{\partial (\rho v)}{\partial y} + \frac{\partial (\rho w)}{\partial z} = 0$$

Navier-Stokes:
$$\rho \frac{Du}{Dt} = X - \frac{\partial P}{\partial x} + \frac{\partial}{\partial x} \left[\mu \left(2 \frac{\partial u}{\partial x} - \frac{2}{3} \text{div } \vec{w} \right) \right] + \frac{\partial}{\partial y} \left[\mu \left(\frac{\partial u}{\partial y} + \frac{\partial v}{\partial x} \right) \right] + \frac{\partial}{\partial z} \left[\mu \left(\frac{\partial w}{\partial x} + \frac{\partial u}{\partial z} \right) \right]$$

$$\rho \frac{Dv}{Dt} = Y - \frac{\partial P}{\partial y} + \frac{\partial}{\partial y} \left[\mu \left(2 \frac{\partial v}{\partial y} - \frac{2}{3} \text{div } \vec{w} \right) \right] + \frac{\partial}{\partial z} \left[\mu \left(\frac{\partial v}{\partial z} + \frac{\partial w}{\partial y} \right) \right] + \frac{\partial}{\partial x} \left[\mu \left(\frac{\partial u}{\partial y} + \frac{\partial v}{\partial x} \right) \right]$$

$$\rho \frac{Dw}{Dt} = Z - \frac{\partial P}{\partial z} + \frac{\partial}{\partial z} \left[\mu \left(2 \frac{\partial w}{\partial z} - \frac{2}{3} \text{div } \vec{w} \right) \right] + \frac{\partial}{\partial x} \left[\mu \left(\frac{\partial w}{\partial x} + \frac{\partial u}{\partial z} \right) \right] + \frac{\partial}{\partial y} \left[\mu \left(\frac{\partial v}{\partial z} + \frac{\partial w}{\partial y} \right) \right]$$

Eqn of State: $P = \rho R_g T$

$$\mu = \mu(P, T)$$

Energy Equation: $\frac{dQ}{dt} = \frac{dE_T}{dt} + \frac{dW}{dt}$

where \vec{w} is the velocity with components u, v, w in respectively the x, y and z direction, $\frac{D}{Dt}$ is the operator $\frac{\partial}{\partial t} + u \frac{\partial}{\partial x} + v \frac{\partial}{\partial y} + w \frac{\partial}{\partial z}$, X, Y and Z are the body forces in

respectively x , y and z directions, P is the local pressure, R_g is the gas constant, Q is the heat into the system, E_T is the internal energy and W is the work done by the system.

Assuming steady state, absence of body forces, viscosity $\mu(T,P)$ is constant, two-dimensional flow, $\frac{\partial P}{\partial y}$ is negligible, laminar flow, and both fluids incompressible (the energy equation decouples), these equations simplify to the Prandtl boundary layer equations:

$$\text{Continuity: } \frac{\partial u}{\partial x} + \frac{\partial v}{\partial y} = 0$$

$$\text{Navier-Stokes: } u \frac{\partial u}{\partial x} + v \frac{\partial u}{\partial y} = - \frac{1}{\rho} \frac{\partial P}{\partial x} + \nu \frac{\partial^2 u}{\partial y^2}$$

Using the subscript g for properties of the inner fluid and the subscript L for the outer fluid, it is possible to write two sets of equations describing the two-fluid laminar boundary layer.

$$\text{Inner fluid: } \frac{\partial u}{\partial x} + \frac{\partial v}{\partial y} = 0 \quad (1)$$

$$u \frac{\partial u}{\partial x} + v \frac{\partial u}{\partial y} = - \frac{1}{\rho} \frac{\partial P}{\partial x} + \nu_g \frac{\partial^2 u}{\partial y^2} \quad (2)$$

$$\text{Outer fluid: } \frac{\partial u}{\partial x} + \frac{\partial v}{\partial y} = 0 \quad (3)$$

$$u \frac{\partial u}{\partial x} + v \frac{\partial u}{\partial y} = - \frac{1}{\rho} \frac{\partial P}{\partial x} + \nu_L \frac{\partial^2 u}{\partial y^2} \quad (4)$$

To describe the problem fully, however, it is required to state the boundary conditions and the conditions at the interface between the two fluids. At the wall, in the inner

fluid, the velocity parallel to the wall, u , is zero (no slip) and the velocity perpendicular to the wall is equal to the imposed blowing velocity. At the interface the tangential velocity and shear stress have to be continuous. Furthermore, the mass transfer across the interface is assumed to be zero. In the outer fluid u has to approach $U(x)$ as y approaches infinity. A formal statement of these conditions is:

$$\text{at } y = 0 \quad u = 0$$

$$v = v_w$$

$$\text{at interface} \quad u_g = u_L$$

$$\mu_g \left(\frac{\partial u_g}{\partial y} \right)_i = \mu_L \left(\frac{\partial u_L}{\partial y} \right)_i$$

$$\dot{m} = 0 \text{ or } v_g (\text{interface}) = v_L (\text{interface}) = 0$$

in outer fluid $u \rightarrow U(x)$ as $y \rightarrow \infty$

For the given assumptions, equations 1-4 and the boundary conditions describe the problem completely. This system presents substantial difficulties in attempting a general solution. Similarity solutions, however, will solve the deadlock.

B. TRANSFORMED EQUATIONS

Similarity-type solutions are well known and have the characteristic that the velocity profiles have similar shapes at all x -positions along the surface. Mathematically this gives the enormous simplification that the governing partial

differential equations are converted into ordinary differential equations. Before defining the dimensionless parameters it should be noted that the continuity equations are satisfied by the stream-function ψ defined by

$$u = \frac{\partial \psi}{\partial x} \text{ and } v = - \frac{\partial \psi}{\partial x}$$

Following Schlichting [12], the following dimensionless parameters can be introduced for the inner fluid:

$$\text{Reynolds number } Re_g = \frac{U_\infty L}{\nu_g} \quad (\text{where } U_\infty \text{ and } L \text{ are some reference quantities})$$

$$\eta_g = \frac{y/\sqrt{Re_g}}{Lg(x)} \quad \xi_g = \frac{x}{L} \quad (\text{where } g(x) \text{ is a dimensionless scale factor for } y)$$

$$f(\eta_g, \xi_g) = \frac{\psi(x, y) \sqrt{Re_g}}{L U(x) g(x)} \quad \text{or} \quad \psi(x, y) = f(\eta_g, \xi_g) \frac{L U(x) g(x)}{\sqrt{Re_g}}$$

To simplify further manipulation, it is wise to state at this point that to ensure similarity $f(\eta_g, \xi_g)$ can not depend on $\xi_g = \xi_g(x)$ so that $f = f(\eta_g)$.

From the above, the velocity components may be derived,

$$u = U(x) f'(\eta_g)$$

$$\text{and } v = - \frac{L f(\eta_g)}{\sqrt{Re_g}} \frac{d}{dx} (U(x) g(x)) + \frac{L U(x) g(x)}{\sqrt{Re_g}} \eta_g f_g'(\eta_g) \frac{d}{dx} g(x)$$

Inserting these expressions into the Prandtl boundary layer equation and after a considerable amount of algebra the equation converts into

$$f_g'''' + \alpha f_g f_g'' + \beta (1 - f_g'^2) = 0$$

where $\alpha = \frac{L g(x)}{U_\infty} \frac{d}{dx}(U(x) g(x))$

$$\beta = \frac{L g^2(x)}{U_\infty} \frac{dU(x)}{dx}$$

Reasoning in the same way for the outer fluid after defining

$$Re_L = \frac{U_\infty L}{\nu_L} ; \eta_L = \frac{(y - \delta)}{L g(x)} \sqrt{Re_L} , \quad \xi_L = \frac{x}{L}$$

$$f_L(\eta_L, \xi_L) = \frac{\psi(x, y) \sqrt{Re_L}}{L U(x) g(x)}$$

one arrives at

$$f_L'''' + \alpha f_L f_L'' + \beta (1 - f_L'^2) = 0$$

where α and β are defined the same as for the inner fluid.

It should be noted that to satisfy the similarity requirement α and β should not depend on x . Still following Schlichting [12], it is possible to arrive at the following general conditions for $U(x)$ and $g(x)$:

$$\frac{U(x)}{U_\infty} = K^{\frac{2}{2\alpha-\beta}} \left[(2\alpha - \beta) \frac{x}{L} \right]^{\frac{\beta}{2\alpha-\beta}} \quad \text{where } K \text{ is an integration constant}$$

$$g(x) = \sqrt{(2\alpha - \beta) \frac{x}{L} \frac{U_\infty}{U(x)}}$$

Now, without loss of generality, take $\alpha = 1$ and introduce a new constant $m = \frac{\beta}{2-\beta}$ so that the expressions for $\frac{U(x)}{U_\infty}$ and $g(x)$ convert to

$$\frac{U(x)}{U_\infty} = K^{(1+m)} \left(\frac{2}{1+m} \frac{x}{L} \right)^m$$

$$g(x) = \sqrt{\frac{2}{m+1} \frac{x}{L} \frac{U_\infty}{U(x)}}$$

Furthermore, the transformation equations for the ordinates are $\eta_g = y \sqrt{\frac{m+1}{2} \frac{U(x)}{v_g x}}$ and $\eta_L = (y-\delta) \sqrt{\frac{m+1}{2} \frac{U(x)}{v_L x}}$

With Schlichting [12], it can be noted that these requirements can be satisfied by the flow in the neighbourhood of the stagnation point of a wedge with included angle $\beta\pi$, where $U(x)$ is given by Cx^m .

Next the boundary and interface conditions have to be converted by expressing them into the newly defined dimensionless parameters

At $y = 0$

$$\text{or } \eta_g = 0 \quad u = U(x) \quad f_g'(\eta) = 0 \quad \text{or } f_g'(0) = 0$$

$$v = v_w = \frac{-L f_g(\eta_g)}{\sqrt{Re}} \frac{d}{dx}(U(x) g(x))$$

$$\text{or } f_g(\eta_g) = \frac{-v_w \sqrt{Re_g}}{L \frac{d(U(x) g(x))}{dx}}$$

$$\text{at interface } \eta_g = \eta_{gi} \quad \dot{m} = 0 \quad \text{or } f_g(\eta_{gi}) = f_L(0) = 0$$

$$\eta_L = 0$$

$$u_g = u_L \quad \text{or } f_g'(\eta_{gi}) = f_L'(0)$$

$$\mu_g \frac{du_g}{dy} = \mu_L \frac{du_L}{dy} \quad \text{or } f_g''(\eta_i) = R f_L''(0) \quad \text{where } R = \left\{ \frac{(\rho\mu)_L}{(\rho\mu)_g} \right\}^{\frac{1}{2}}$$

$$\text{for } y \rightarrow \infty \quad \text{or } \eta_L \rightarrow \infty \quad u \rightarrow U(x) \quad \text{or } f_L' \rightarrow 1 \quad \text{as } \eta_L \rightarrow \infty.$$

It should be noted that

- to ensure that $f_g(\eta_g)$ is independent of x :

$$v_w \sim \frac{d(U(x) g(x))}{dx} . \quad \text{Inserting the expressions for } U(x)$$

$$\text{and } g(x) \text{ one obtains } v_w \sim \sqrt{\frac{x}{U(x)}}$$

- R depends on the properties of both fluids depending on temperature and pressure.

Summarizing the problem can be formally stated by

$$\text{equations: } f_g''' + f_g f_g'' + \beta(1 - f_g'^2) = 0 \quad (5a)$$

$$f_L''' + f_L f_L'' + \beta(1 - f_g'^2) = 0 \quad (5b)$$

$$\text{and conditions: } f_g'(0) = 0$$

$$f_g(0) = -v_w \sqrt{\frac{2x}{(m+1) v_g U(x)}} \text{ where } v_w \sim \sqrt{\frac{U(x)}{x}}$$

$$f_g(\eta_{gi}) = f_L(0) = 0$$

$$f_g'(\eta_{gi}) = f_L'(0)$$

$$f_g''(\eta_{gi}) = R f_L''(0)$$

$$f_L'(\eta_L + \infty) = 1$$

IV. EXPLORED WAYS OF SOLUTION

A. SERIES SOLUTION

Following the procedure of Sparrow, Jonsson and Eckert [7], a series solution of the momentum equation seems to be appropriate. Expanding $f_g(\eta_g)$ with respect to $\eta_g = 0$ gives

$$f_g(\eta_g) = f_g(0) + f_g'(0)\eta_g + \frac{f_g''(0)\eta_g^2}{2!} + \frac{f_g'''(0)\eta_g^3}{3!} + \dots$$

The first two terms in the expansion are available from the boundary conditions. The $f_g''(0)$ is unknown for now and will be determined by the solution. Higher derivatives can be expressed in terms of lower derivatives by taking sequentially derivatives of both sides of the momentum equation

$$f''' = -f f'' - \beta(1 - f'^2)$$

and evaluating at $\eta_g = 0$.

Some expressions for derivatives are:

$$f^{(III)}(0) = -f(0)f''(0) - \beta$$

$$f^{(IV)}(0) = f^2(0)f''(0) + \beta f(0)$$

$$f^{(V)}(0) = -f^3(0)f''(0) - \beta f^2(0) + (2\beta - 1)f''^2(0)$$

$$f^{(VI)}(0) = f^4(0)f''(0) + \beta f^3(0) - (8\beta - 5)f(0)f''^2(0) \\ - (6\beta - 4)\beta f''(0)$$

It was impossible to find a recurrency in the expressions. On applying the interface condition $f(\eta_{gi}) = 0$ makes it possible to write

$$f_g''(0) = \frac{-f(0)}{\frac{1}{2}\eta_{gi}^2 + \sum_{k=3} \frac{f_g^{(k)}(0)\eta_{gi}^k}{f_g''(0)k!}}$$

It is now possible to express $f_g''(0)$ in liquid and gas parameters. Here Sparrow, Jonsson and Eckert refer to an earlier paper by Cess and Sparrow [3]. This paper is discussed in Chapter II, Section A3. This paper gives a table relating $f_L'(0)$ and $f_L''(0)$ which corresponds to a solution of the equation for a flat plat.

At this point it was realized that the data necessary to go any further was not available, therefore this method was abandoned, and other methods of solution were explored.

B. NUMERICAL SOLUTIONS

1. IODE [13]

IODE is an interactive ordinary differential equation solver developed by the Computer Center of the Naval Postgraduate School. The program accepts a number of first order non-linear ordinary differential equations with associated initial conditions and solves the equations.

In this case equations 5 were converted into:

$$\frac{dy_1}{d\eta} = y_2 = f' \quad \text{Note: } y_1 = f \quad (6a)$$

$$\frac{dy_2}{d\eta} = y_3 = f'' \quad (6b)$$

$$\frac{dy_3}{d\eta} = f''' = -y_1 y_3 - \beta + \beta y_2^2 \quad (6c)$$

where y_1 , y_2 and y_3 are dummy variables for the derivatives of $f(\eta)$, with initial conditions

$$y_1(0) = f(0) \quad (7a)$$

$$y_2(0) = f'(0) \quad (7b)$$

$$y_3(0) = f''(0) \quad (7c)$$

The equations 6 are the same for both fluids but as noted before the initial conditions differ.

Sanders [14] suggested that it should be possible to guess the thickness of the inner fluid layer η_{gi} and then a value of $f_g''(0)$ could be found by trial and error so that no mass transfer occurs across the interface ($f_g(\eta_{gi}) = 0$). The values for f_g , f_g' and f_g'' at the interface give the initial conditions for the outer fluid equations 6. The values of $f_L'(\eta_L)$ should approach unity for large enough η_L while $f_L''(\eta_L)$ approaches 0. If $f_L'(\eta_L)$ does not go to unity the initial guess for the layer thickness was wrong and another value for the inner fluid layer thickness η_{gi} is chosen. This process is repeated until a layer thickness is found for which $f_L'(\infty) = 1$ and $f_L''(\infty) = 0$.

The calculations carried out on the IBM 3033AP computer system showed that this procedure worked, but while the

calculations were fast the interactive side of the program has proven to be too time consuming.

2. Desk Top Computer

So the necessity arose to find some way to decrease the time spent communicating with the computer and to automate the trial and error process. Furthermore, it was necessary to find some way to interrupt the execution and to execute the program by steps to determine instabilities in the solution.

Since a Wang 2200 desk-top computer with line printer was available, the problem was rewritten for this computer and the solution for a number of cases was carried out. It has to be realized that a desk-top computer is relatively slow so that a compromise between calculation time and accuracy of the result had to be found. It was decided that the primary goal was to find a method of solution and not to tabulate a large amount of accurate data. In the light of all the assumptions high accuracy would be doubtful anyway.

V. SOLUTIONS

A. DEFINITION OF THE PROBLEM

The momentum equation will be written as three first order differential equations as for the "IODE program":

$$\frac{dy_1}{dn} = y_2 = f'$$

$$\frac{dy_2}{dn} = y_3 = f''$$

$$\frac{dy_3}{dn} = -y_1 y_3 - \beta - \beta y_1^2$$

Now multiplying both sides of these equations by dn and changing to finite differences one arrives at

$$\Delta y_1 = y_2 \cdot \Delta n$$

$$\Delta y_2 = y_3 \cdot \Delta n$$

$$\Delta y_3 = (-y_1 \cdot y_3 - \beta - \beta y_1^2) \cdot \Delta n$$

Now by stepping n through the desired range of values, starting with known or guessed initial values for η_0 , y_1 , y_2 and y_3 it is possible to calculate y_1 , y_2 and y_3 as a function of η .

It has to be noted at this point that we approximate the integrals by a "Lower Riemann Sum". It is known, however, that using a "sufficient" number of steps guarantees a satisfactory accuracy. This procedure is applicable for both the inner and the outer fluid. The initial values for the outer

fluid follow logically from the solution of the inner fluid and the interface conditions.

Given values for the blowing parameter $f_g(0)$ and the properties of the fluids parameter R the procedure is as follows:

- Choose an inner fluid layer thickness.
- Find $f''(0)$ by an interval halving method so that $f(\eta_{gi})$ (no mass transfer across the interface) equals 0, or g_i in our program is smaller than a chosen value.

Note: $f(0) = \text{given}$; $f'(0) = 0$ and $f''(0)$ is chosen as indicated.

- Apply the interface conditions on the values for f , f' and f'' at the interface to find the initial values for the solution of the outer fluid equations. Choose an end value for η_L large enough to be well "outside" the boundary layer.
- Check if $f_L'(\infty) = 1$ but also if $f_L''(\infty) \approx 0$ as it is possible that an unstable solution is found. In case the conditions are satisfied the solution is found. If not another guess on the inner fluid layer thickness has to be made.
- The value of the inner fluid layer thickness is chosen in another interval halving process.
- This process is repeated until the requirements of $f_L'(\infty) = 1$ and $f_L''(\infty) \approx 0$ are met.

A copy of this program is enclosed as Appendix A.

From the above, it follows that the initial intervals for $f_g''(0)$ and η_{gi} have to be determined. The interval for η_{gi} should be as narrow as possible and the interval for $f''(0)$ should be a little wider than expected to prevent instabilities and "limit-riding". These values were determined by trial and error and the results are discussed in a later chapter.

B. TESTING THE PROGRAM

1. Number of Steps of Independent Variable

The program is used with 100 steps of the independent variable. A sample problem was solved with both 100 and 200 steps. The deviations were in the fourth decimal (see Table 5.1). The time required for the calculation however was doubled from approximately 45 minutes to 90 minutes.

2. One Fluid Flow

It is clear that when R approaches unity, the two fluids are hydrodynamically identical. Computer solutions were obtained for a single fluid flow for $\beta = 0$ (flat plate) and $\beta = 1$ (stagnation flow) and further for $\beta = 0.2, 0.4, 0.6$ and 0.8 . The results were in good agreement with Nickel [5], "abbildung 8". (See Table 5.2.)

3. Solution for R Close to 1

A solution with a R of 1.1 was compared to that for a one-fluid problem and the results were close enough to give further confidence in the correctness of the program to handle non-unity values of R . (See Table 5.3.)

4. Solution for Small Wedge Angles

The solution for a β of 0.01 was close enough to that of the flat plate to give confidence about the capabilities of the program to correctly handle non-zero values of β . (See Table 5.4.)

VI. RESULTS

A. DEFINITION OF A SAMPLE PROBLEM

To demonstrate the capabilities of the program, a special case was chosen for thorough investigation. For this case, "air at standard conditions" and water were chosen as the two fluids so that $R = 200$. For a range of blowing parameters $f_g(0)$, and wedge angles β , the velocity profile was calculated and the layer thickness η_{gi} of the inner fluid and the shear stress parameter $f_g''(0)$ at the wall were determined.

B. THICKNESS OF THE INNER FLUID LAYER

Figure 6.1 gives the dimensionless thickness of the inner fluid layer η_{gi} as a function of the blowing parameter $f_g(0)$ for various wedge angles β . Figure 6.2 is an enlargement of these curves for small blowing-parameters. These graphs lead to the following observations:

- For small values of the blowing parameter the curves are straight lines, η_{gi} decreases very little with increasing wedge angle and is directly proportional to $f_g(0)$.
- For larger blowing parameters $f_g(0)$, η_{gi} increases more rapidly with increasing $f_g(0)$. For large blowing parameters and small angles the thickness of the inner fluid layer increases drastically with increased blowing parameter.
- For large values of the blowing parameter, the thickness of the inner fluid layer decreases rapidly with increasing wedge angle β .

C. WALL SHEAR STRESS

Figures 6.3 and 6.4 give the dimensionless wall shear stress $f_g''(0)$ as a function of the blowing parameter $f(0)$ and the wedge angle β .

- For all values of wedge angle β , blowing decreases the wall shear stress $f_g''(0)$. This reduction is spectacular for small values of the blowing parameter; e.g. for both the flat plate ($\beta = 0$) and stagnation flow ($\beta = 1$) $f_g''(0)$ is reduced to half the non-blowing value when $f_g(0) = 0.0025$.
- For all values of the blowing parameter the wall shear stress $f''(0)$ increases with increasing wedge angle β ; the smaller thickness of the inner fluid layer caused by the higher potential velocity.
- For large values of the blowing parameter, the wall shear stress is very small and nearly equal for all wedge angles. The values obtained indicate that the wall shear stress for large blowing parameters approaches the wall shear stress for a wedge in an infinite volume of inner fluid. (See Table 6.1.)

D. VELOCITY PROFILES

Figure 6.5 gives velocity profiles ($f'(\eta)$ vs. η) for various blowing parameters for a wedge angle $\beta = 0.2$ (36°). The η_L and η_g have been expressed in the same relative scale by noting that $\eta_g = \frac{y\sqrt{Re_g}}{L g(x)}$ and $\eta_L = \frac{(y-\delta)\sqrt{Re_L}}{L g(x)}$ resulting in

$$\frac{\Delta \eta_g}{\Delta \eta_L} = \frac{1}{3}.$$

The following observations can be made:

- For the smaller blowing parameters the velocity profiles in the inner fluid are nearly straight lines.
- The stronger the blowing the thicker the layer of the inner fluid causing a larger proportion of the potential velocity to be obtained in the inner fluid layer. For

small blowing parameters this proportion of the potential velocity increases rapidly with increasing blowing parameter. Figure 6.6 gives the proportion of the potential velocity (or $f_g'(\eta_{gi})$) as a function of the blowing parameter $f_g(0)$.

- Particularly interesting is the fact that the velocity profiles in the inner fluid and the outer fluid have opposite curvatures. This is comparable to the boundary layers associated with the gas-filled cavity attached to a body after water entry. The cavity around such a body has a stable interface; breakdown occurs only when too much gas is left at the rear separation. Although no rigorous proof can be given it is felt that this characteristic of the velocity profile provides stability of the interface in two fluid boundary layer flow.

E. DRAG REDUCTION

To characterize the amount of drag reduction, the local drag parameter $f_g''(0)$ obtained for the two fluid flow was compared to the local drag parameter obtained without blowing.

To compare these local drags, a minor conversion has to be made. The shear stress at the wall is

$$\tau = \mu \left(\frac{du}{dy} \right)_{y=0}$$

In terms of the transformed variables, the expression for τ becomes

$$\tau = \mu_g \frac{U(x)}{L g(x)} \sqrt{Re_g} (f_g''(\eta))_{\eta=0}$$

which can be expressed in the outer fluid parameters

$$\tau = \mu_L \frac{U(x)}{L g(x)} \sqrt{Re_L} \left\{ \frac{(\rho\mu)_g}{(\rho\mu)_L} \right\}^{\frac{1}{2}} \cdot f_g''(\eta)$$

For the outer fluid, without blowing, the reference shear stress τ_0 is:

$$\tau_0 = \mu_L \frac{U(x)}{g(x)} \sqrt{Re_L} (f_L''(\eta))_{\eta=0} \quad f_g(0)=0$$

Now taking the ratio:

$$\frac{\tau}{\tau_0} = \frac{f_g''(0)}{R(f_L''(0))} f_g(0) = 0$$

The values of this reference shear stress parameter $f_L''(0)$ are calculated and reflected in Figure 6.7. Since R is a known constant, for each value of the shear stress parameter $f_g''(0)$ it is possible to determine the ratio τ/τ_0 . Table 6.2 gives the values of τ/τ_0 as a function of wedge angle β and blowing parameter $f_g(0)$ for $R = 200$.

Inspection of this table reveals that a drag reduction is observed for all blowing parameters and wedge angles. It is remarkable that for small values of the blowing parameter the ratio τ/τ_0 decreases for increasing wedge angle β while for large values of the blowing parameter $f(0)$ the ratio τ/τ_0 increases with increasing wedge angle β . For all wedge angles β , however, the ratio τ/τ_0 decreases with increasing blowing strength.

F. REQUIRED POWER

The power required to maintain blowing is

$$\text{Power} = P \cdot v_w$$

where P is the local pressure given by

$$P = P_{\text{STAG}} + \left(\frac{\partial P}{\partial x} \right) dx$$

where P_{STAG} is the stagnation pressure at the leading edge of the wedge and $\frac{\partial P}{\partial x} = -\rho_g U \frac{dU}{dx} = -\rho_g C^2 m x^{2m-1} < 0$. If the inner fluid is at stagnation pressure P_{STAG} a pressure difference of $\frac{\partial P}{\partial x}$ at the wall exists so that the fluid flows out by itself. The flow rate then can be controlled by the blowing hole's size. Of course, the ejected fluid has to be replaced requiring it to be brought up to P_{STAG} . In practice this is of less interest as a considerable amount of exhaust gases of the propulsion systems at high pressures should be available.

VII. CONCLUSIONS AND RECOMMENDATIONS

It has been shown theoretically that a dramatic drag reduction is possible for the infinite wedge by blowing with a lighter and less viscous fluid, and that the parameters involved can be calculated with relatively simple means. Furthermore the developed method gives another way of solving the flat plate case and the stagnation flow case.

This work directly invites a number of follow-on investigations of phenomena associated with:

- finite two-dimensional bodies
- three-dimensional bodies
- a compressible inner fluid
- experimental verification of the theory
- stability of the interface

all of equal importance.

APPENDIX A

"BASIC" PROGRAM FOR WANG DESK TOP COMPUTER TO SOLVE TWO FLUID LAMINAR FLOW CHARACTERISTICS

```

1  REM THIS PROGRAM IS DESIGNED TO CALCULATE F,F',F"
2  REM AND NGI FOR A TWO-LIQUID-LAMINAR-BOUNDARY-LAYER
3  REM GIVEN A BLOWING-PARAMETER F(0),A WEDGEANGLE B AND
4  REM A LIQUID-PROPERTIES-CONSTANT R.
5  REM
6  REM TO USE THE PROGRAM ONE HAS TO GUESS ON AN INITIAL
7  REM INTERVAL FOR THE INNER-FLUID-LAYER-THICKNESS AND
8  REM FOR THE LOCAL SHEARSTRESS-PARAMETER F"(0).THESE
9  REM VALUES CAN BE OBTAINED FROM GRAPHS IN THE THESIS.
10 REM ONE HAS TO TAKE THE INTERVAL FOR THE THICKNESS AS
11 REM SMALL AS POSSIBLE AND THE INTERVAL FOR THE SHEAR-
12 REM STRESS A LITTLE BIT LARGER THAN EXPECTED TO PREVENT
13 REM INSTABILITIES AND LIMITRIDING.
14 REM
15 REM IN SHORT INSERT VALUES FOR
16 REM - F(0) AS G1(1),LOWER LIMIT OF F"(0) AS G6 AND
17 REM - UPPER LIMIT OF F"(0) AS G7 IN LINE 120
18 REM - LOWER LIMIT OF NGI AS H6 AND UPPER LIMIT OF
19 REM - NGI AS H7 IN LINE 130
20 REM - WEDGE ANGLE B AND FLUID PROPERTIES CONSTANT R
21 REM - IN LINE 140
22 REM
23 REM THE OUTPUT WILL CONSIST OF TWO TABLES GIVING
24 REM FG,FG',FG",FL,FL' AND FL" AS A FUNCTION OF THE
25 REM DIMENSIONLES PARAMETERS NG AND NL,PLUS A HEADING
26 REM OF THE MOST IMPORTANT PARAMETERS AND CONSTANTS.
27 REM
28 REM
100 DIM G0(101), G1(101), G2(101), G3(101)
105 DIM L0(101), L1(101), L2(101), L3(101)
110 G0(1)=0: G1(1)=-.5: G2(1)=0: G6=0: G7=2
115 H6=.95: H7=1.05
120 G4=G6: G5=G7
125 A=1: B=1: R=200
130 Z=0: Z1=0
135 H8=H6: H9=H7
140 H=(H8+H9)/2
145 G8=G6: G9=G7
150 G3(1)=(G8+G9)/2
155 IF H=0 THEN 400
160 IF Z < 35 THEN 180

```

```

165 PRINT "AFTER 35 ITERATIONS IN GAS UNABLE TO MEET REQ'S"
170 PRINT H,G1(101),G2(101),G3(1)
175 GOTO 495
180 H0=H/100
185 FOR I=1 TO 100
190     H1=G2(I)*H0
195     H2=G3(I)*H0
200     H3=H0*(B*G2(I)*G2(I)-B-A*G1(I)*G3(I))
205     G1(I+1)=G1(I)+H1
210     G2(I+1)=G2(I)+H2
215     G3(I+1)=G3(I)+H3
220     G0(I+1)=G0(I)+H0
225 NEXT I
230 Z=Z+1
235 IF ABS(G1(101)) < .00000001 THEN 255
240     IF G1(101) > 0 THEN 250
245     G8=G3(1): GOTO 150
250     G9=G3(1): GOTO 150
255 L0(1)=0: L1(1)=G1(101): L2(1)=G2(101): L3(1)=G3(101)/R
260 M=10
265 M0=M/100
270 FOR I=1 TO 100
275     M1=L2(I)*M0
280     M2=L3(I)*M0
285     M3=M0*(B*L2(I)*L2(I)-B-A*L1(I)*L3(I))
290     L1(I+1)=L1(I)+M1
295     L2(I+1)=L2(I)+M2
300     L3(I+1)=L3(I)+M3
305     L0(I+1)=L0(I)+M0
310 NEXT I
315 Z1=Z1+1
320 IF Z1 < 35 THEN 335
325 PRINT "AFTER 35 ITERATIONS IN LIQ UNABLE TO MEET REQ'S"
330 GOTO 415
335 C5=L2(101)-1
340 IF H=0 THEN 370
345 IF ABS(L3(101)) > .0001 THEN 355
350     IF ABS(C5) < .00001 THEN 410
355     IF C5 > 0 THEN 365
360         H9=H: G6=G3(1): Z=0: GOTO 140
365         H8=H: G7=G3(1): Z=0: GOTO 140
370 IF ABS(L3(101)) > .0001 THEN 380
375     IF ABS(C5) < .00001 THEN 410
380     IF C5 > 0 THEN 390
385         G8=G3(1): GOTO 395
390         G9=G3(1): GOTO 395
395 G3(1)=(G8+G9)/2
400 L3(1)=G3(1): L0(1)=0: L1(1)=G1(1): L2(1)=L2(1)
405 GOTO 260
410 PRINT "LAMINAR FLOW OVER WEDGE WITH BLOWING"
415 PRINT : PRINT : PRINT .

```

```

420 PRINT "B" = ",B
425 PRINT "R" = ",R
430 PRINT "FG(0)" = ",G1(1),"INITIAL LIMITS : "
435 PRINT "FGDPRIME(0)" = ",G3(1),G4,G5
440 PRINT "NI" = ",GO(101),H6,H7
445 PRINT : PRINT : PRINT
450 PRINT "NG","FG","FGPRIME","FGDPRIME": PRINT
455 FOR I=1 TO 101 STEP 10
460 PRINT GO(I),G1(I),G2(I),G3(I)
465 NEXT I
470 PRINT : PRINT : PRINT
475 PRINT "NL","FL","FLPRIME","FLDPRIME": PRINT
480 FOR I=1 TO 101 STEP 10
485 PRINT LO(I),L1(I),L2(I),L3(I)
490 NEXT I
495 PRINT : PRINT : PRINT : PRINT " ", " ", "END"

```

APPENDIX B

FIGURES

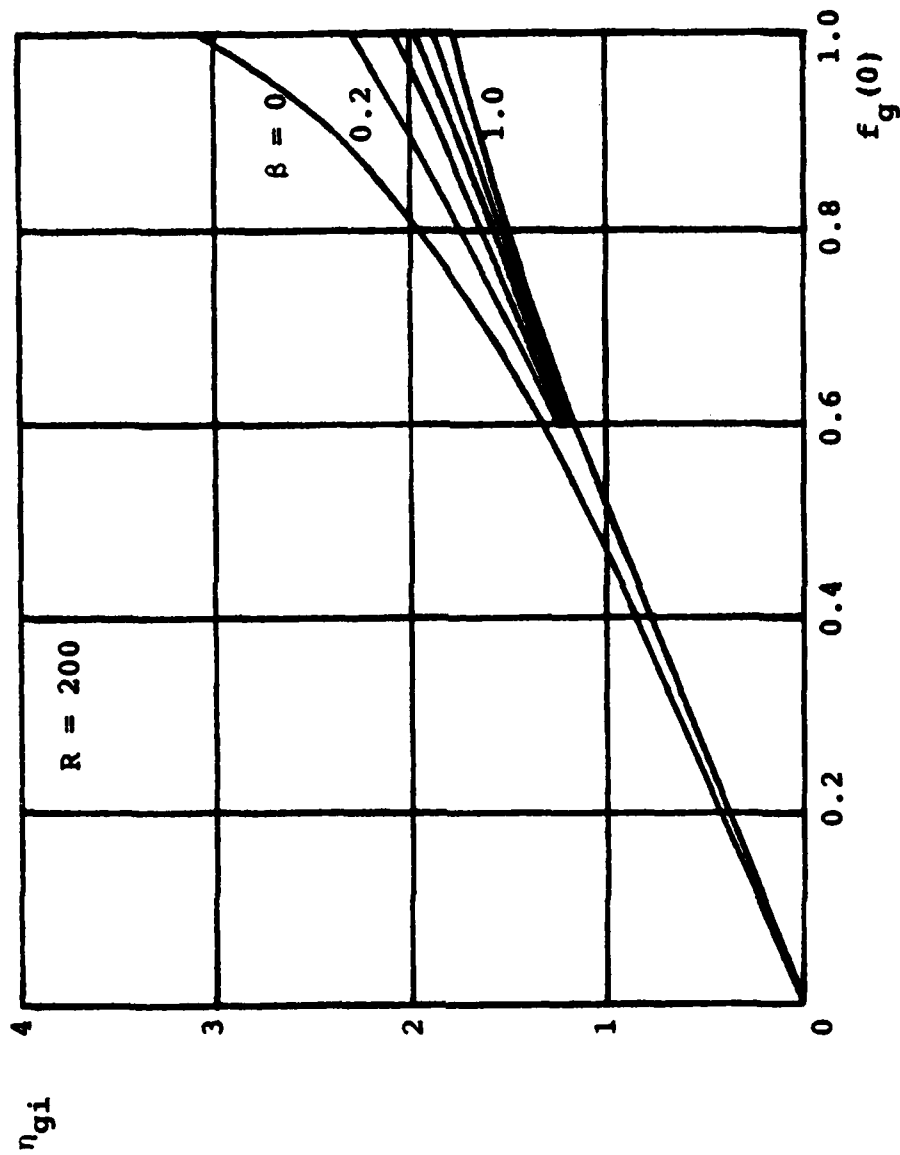


Figure 6.1 Dimensionless inner fluid layer thickness as a function of blowing parameter and wedge angle

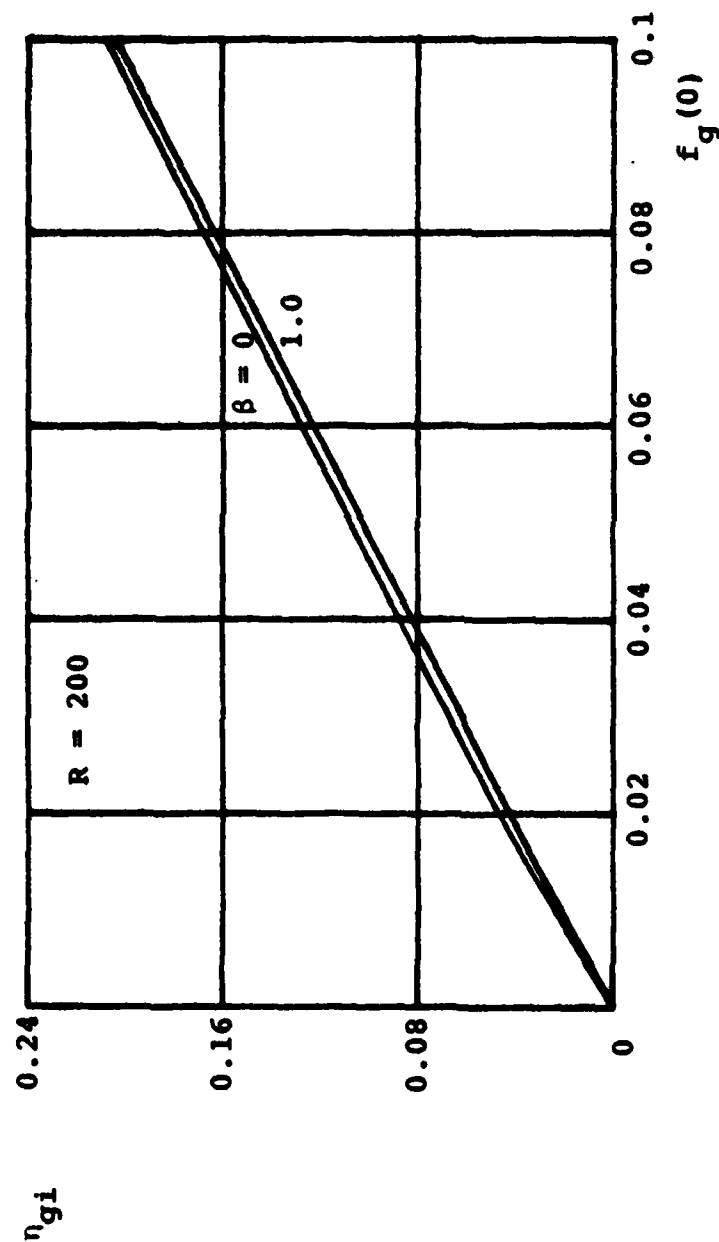


Figure 6.2 Dimensionless inner fluid layer thickness as a function of blowing parameter and wedge angle for small blowing parameters

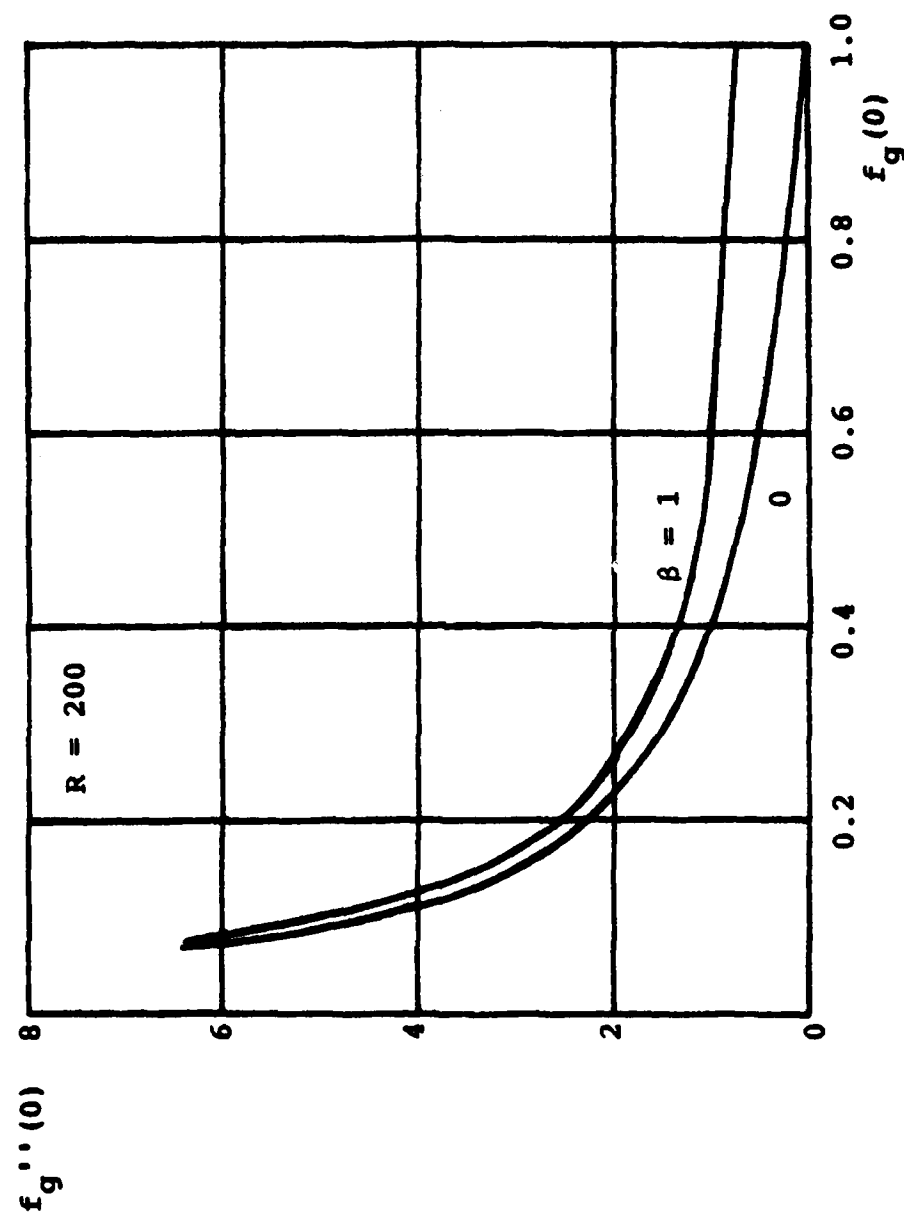


Figure 6.3 Dimensionless wall shear stress as a function of blowing parameter and wedge angle

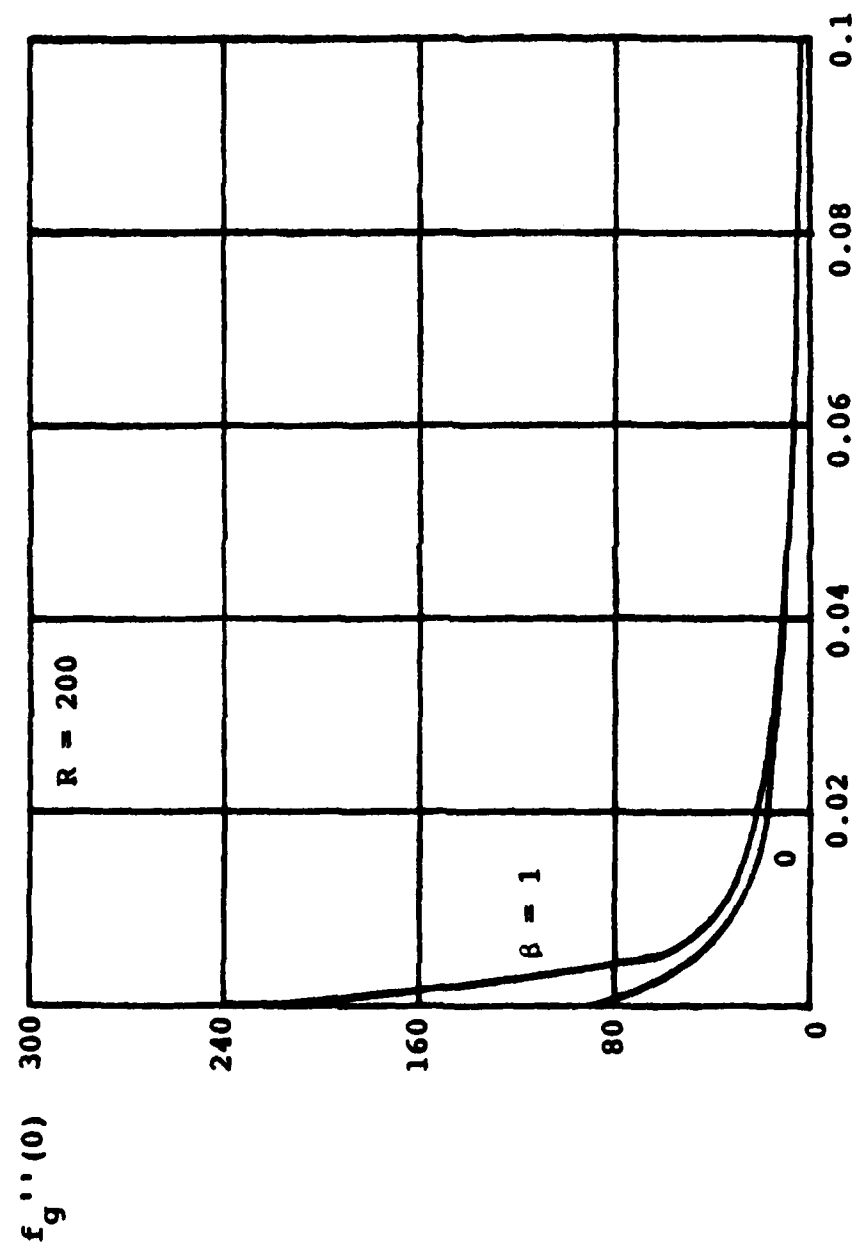


Figure 6.4 Dimensionless wall shear stress as a function of blowing parameter and wedge angle for small blowing parameter

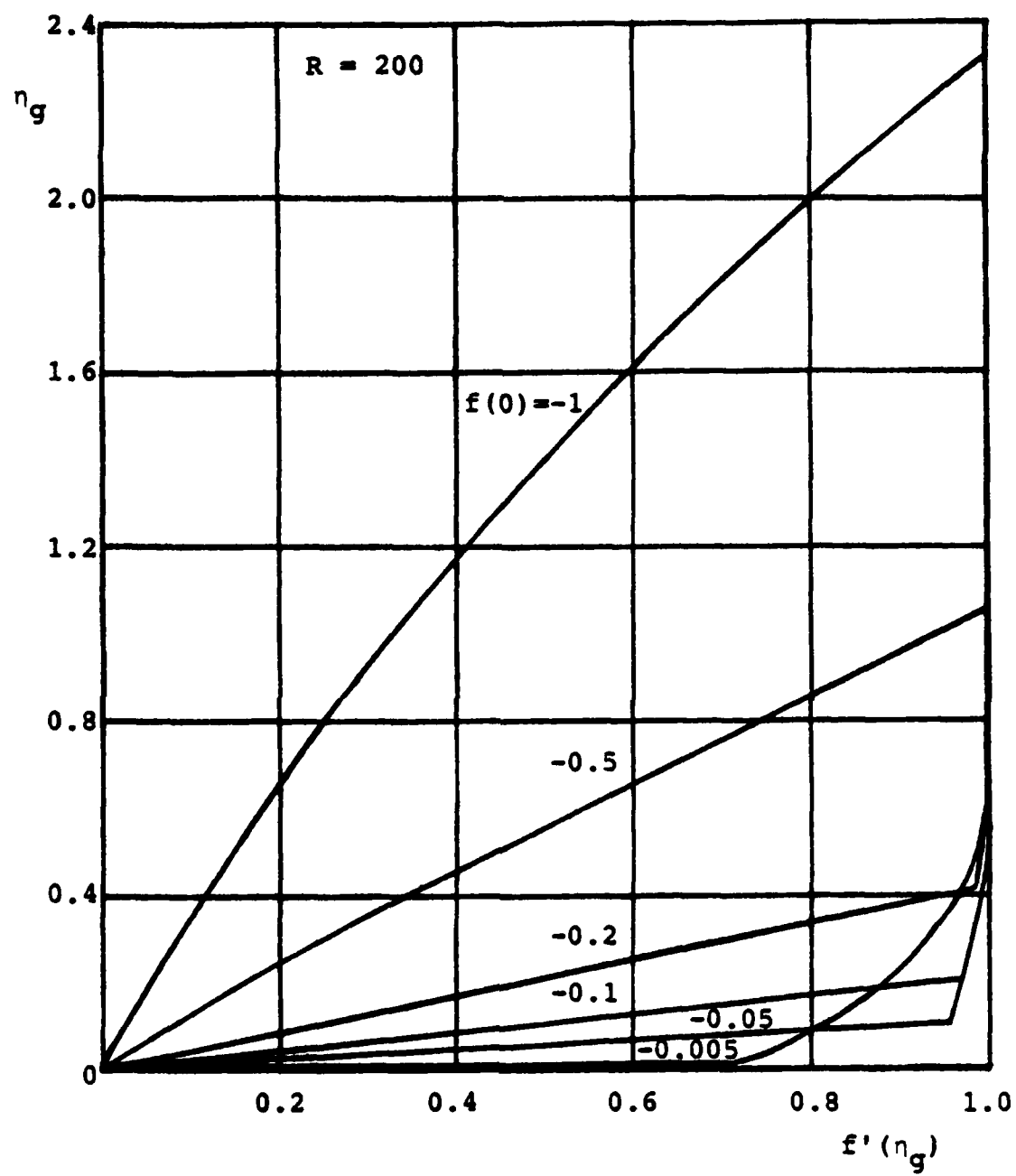


Figure 6.5 Dimensionless velocity profiles

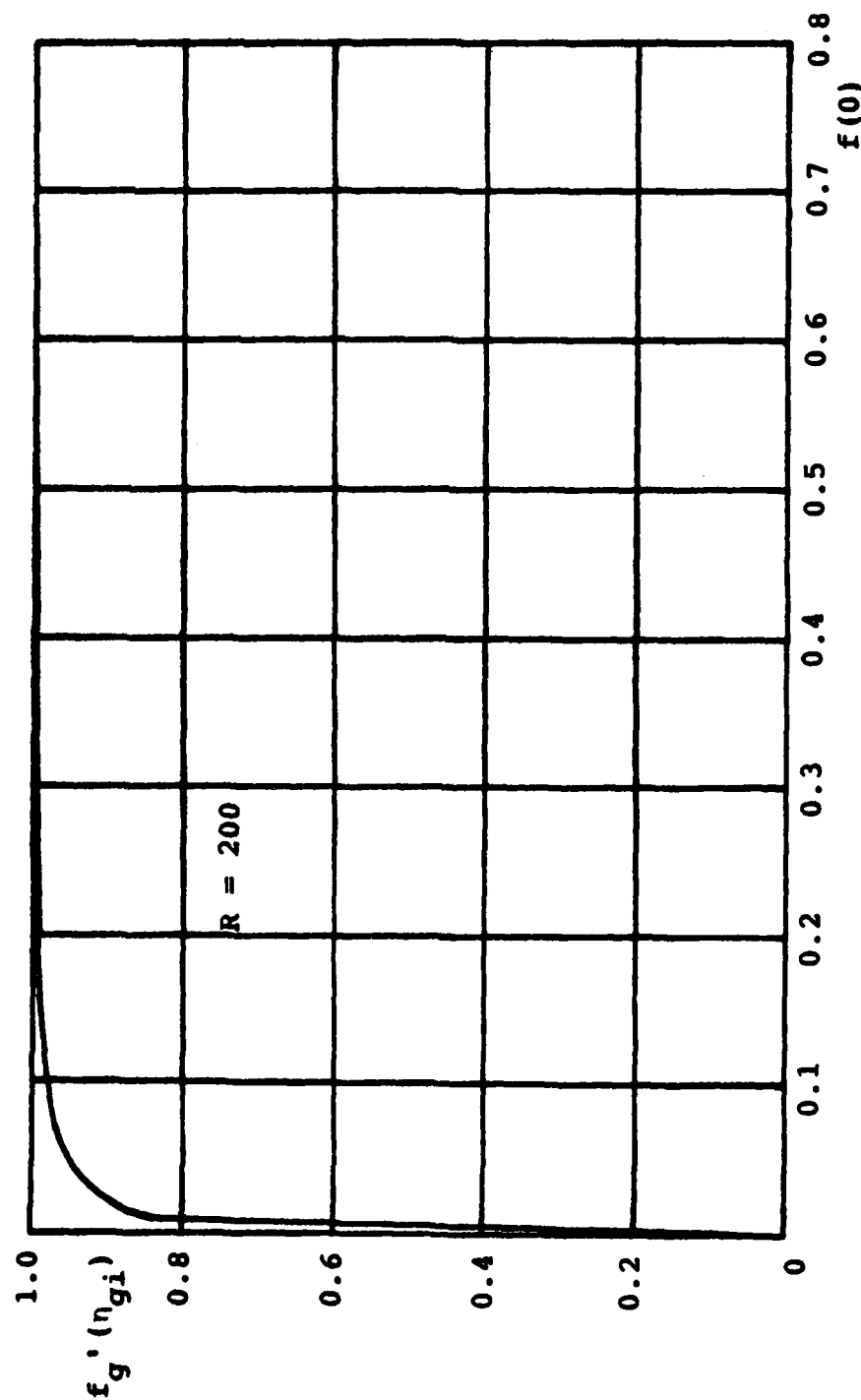


Figure 6.6 Proportion of velocity obtained in the inner fluid layer as a function of blowing parameter

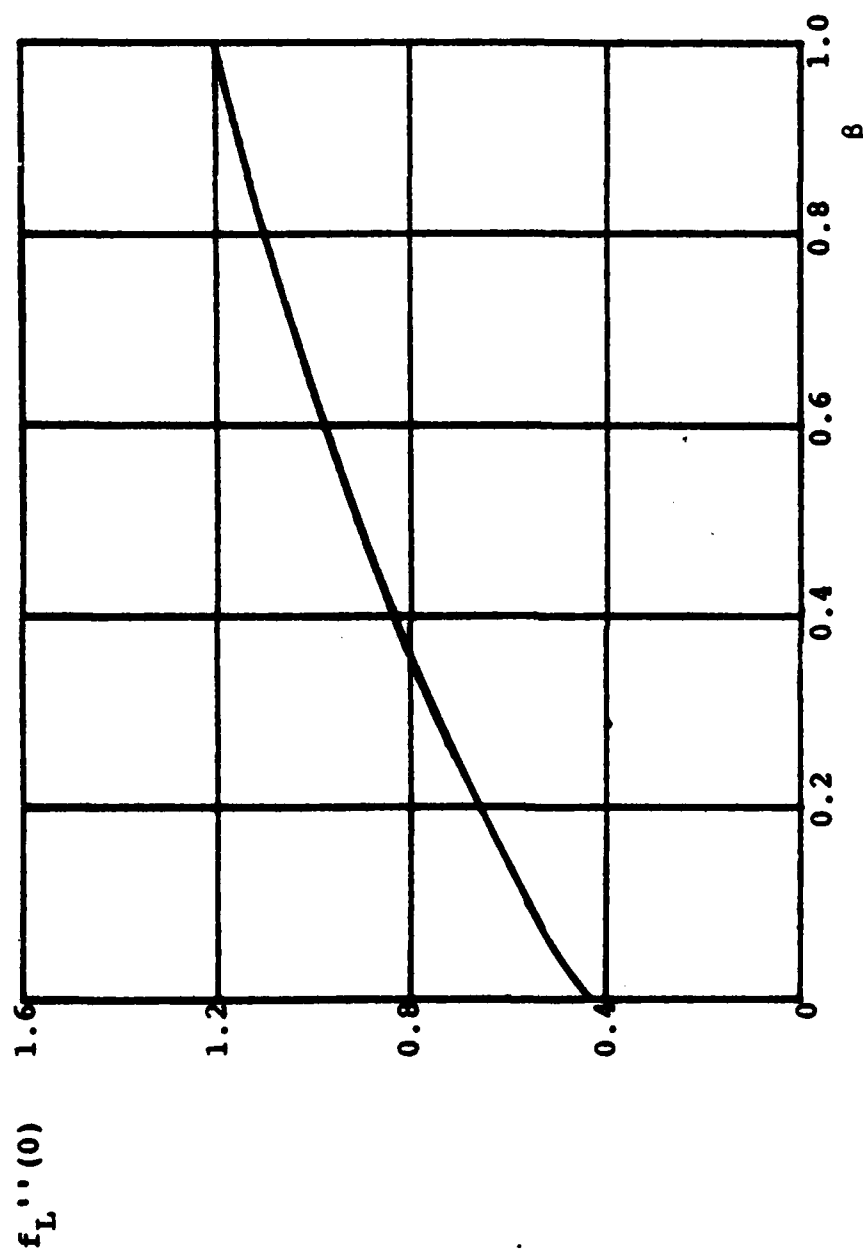


Figure 6.7 Dimensionless wall shear stress for the outer fluid without blowing as a function of the wedge angle

APPENDIX C

TABLES

Table 5.1 Comparison Between 200 and 100 Integration Steps

B	R	FG(0)	FGDPRIME(0)	NI	200 STEPS		INITIAL LIMITS :	
					.5	200	2.29	2.545
					-.2			.415
					2.441610283853			
					.405895996083			

NG	FG	FGPRIME	FGDPRIME
0	-.2	0	2.441610283853
4.05895996E-02	-.1980893802414	9.90948804E-02	2.441139196504
8.11791992E-02	-.1921569061701	.1981707589403	2.440674313966
.121768798827	-.1822033441826	.2972278900133	2.440215793835
.162358398435	-.1682294501986	.3962665361504	2.439763866514
.202947998043	-.1502359692891	.4952869705096	2.439318832267
.243537597651	-.1282236351862	.5942894797317	2.438881057887
.284127197259	-.1021931696857	.6932743665675	2.438450972824
.324716796867	-7.21452819E-02	.7922419523368	2.438023064715
.365306396475	-3.80806676E-02	.8911925791935	2.437615874211
.405895996083	-8.29790000E-09	.9901266121649	2.43721198904

NL	FL	FLPRIME	FLDPRIME
0	-8.29790000E-09	.9901266121649	1.21860599E-02
1	.9945737149788	.997982132458	3.78309479E-03
2	1.993702432642	.9998120062623	5.01385311E-04
3	2.993640251127	.9999953701279	2.52562957E-05
4	3.993641123273	1.000003088699	1.19118190E-06
5	4.993644660373	1.000003974439	7.97887325E-07

Table 5.1 (continued)

B	R	FG(0)	FGDPRIME(0)	NI	100 STEPS		INITIAL LIMITS :	FGDPRIME
					.5	200		
					-.2		2.29	2.545
					2.42941737652			.415
					.4079606933522			

NG	FG	FGPRIME	FGDPRIME
0	-.2	0	2.42941737652
4.07960693E-02	-.1981806177083	9.91001824E-02	2.428848396884
8.15921386E-02	-.1923187605524	.1981774365039	2.42829490893
.1223882080072	-.1824153522746	.2972323983732	2.427757159622
.1631842773422	-.1684712904594	.3962657159258	2.427235478348
.2039803466772	-.1504874459986	.4952780518554	2.426730269232
.2447764160122	-.1284646624329	.5942700865919	2.42624200291
.2855724853472	-.1024037551795	.6932425208544	2.425771207639
.3263685546822	-7.23055106E-02	.7921960778273	2.425318459672
.3671646240172	-3.8170685E-02	.8911315049311	2.424884372865
.4079606933522	-4.81007500E-09	.9900495751529	2.424469587487

NL	FL	FLPRIME	FLDPRIME
0	-4.81007500E-09	.9900495751529	1.21223479E-02
1	.9943601726158	.9980197185913	3.6602193E-03
2	1.993475703139	.9998320514607	4.39633129E-04
3	2.993417621819	.9999959939962	1.70624449E-05
4	3.993417264676	1.000001106507	4.49024329E-07
5	4.99341852912	1.000001430336	2.86762096E-07

Table 5.2 Comparison Between Single Fluid Flow
and Nickel (abb 8) [5]

<u>β</u>	<u>$f_g(0)$</u>	<u>$f_g''(0)$</u>	
		<u>Program</u>	<u>Nickel</u>
0	0	0.4365	0.46
0.25	-.2	0.5888	0.60
0.25	-.5	0.4399	0.44
0.25	-1	0.2644	0.27
0.5	+1	1.5758	1.62

Table 5.3 Comparison Between $R = 1.1$ and Single Fluid Flow

B	R	FG(0)	FGDPRIME(0)	NI	INITIAL LIMITS :	FG	FGPRIME	FGDPRIME
0	1.1	-0.2	0.3401980876924	1.055765380857	0.3	0	3.62598367E-02	0.3401980876924
1	1.07					3.62598367E-02	7.32860121E-02	0.347433398283
2						7.32860121E-02	0.110739997094	0.3546937004036
3						0.110739997094	0.1496023498196	0.3618254318986
4						0.1496023498196	0.1888311441832	0.3686601309326
5						0.1888311441832	0.2287005725644	0.3750151764871
						0.2287005725644	0.2691297393079	0.3806954844855
						0.2691297393079	0.310015819317	0.3854962918232
						0.310015819317	0.3512336911168	0.3892071234014
						0.3512336911168	0.3926361758102	0.3916169869123
						0.3926361758102		0.3925207627222

Table 5.3 (Continued)

[illegible]

Table 5.4 Comparison Between a Small Wedge Angle and a Flat Plate

B	=	0	
R	=	200	
FG(0)	=	-.2	
FGDPRIME(0)	=	2.291294727327	2.545
NI	=	.4147714843712	.415
			INITIAL LIMITS :
			2.29
			.403

NG	FG	FGPRIME	FGDPRIME
0	-.2	0	2.291294727327
4.14771484E-02	-.1982222450625	9.53915943E-02	2.310327755551
8.29542968E-02	-.1924732006161	.1915704820269	2.329175011532
.1244314453122	-.1827204364523	.2885216391343	2.347441570385
.1659085937492	-.168932454383	.3862133790945	2.364717549836
.2073857421862	-.1510793907136	.4845967543127	2.380579442315
.2488628906232	-.12913374233	.5836050284572	2.394592275337
.2903400390602	-.1030711128253	.6831532544908	2.40631264465
.3318171874972	-7.28709735E-02	.7831379952834	2.41529264974
.3732943359342	-3.85174333E-02	.8834372244768	2.421084740622
.4147714843712	-7.40258700E-09	.9839104451743	2.42324745848

NL	FL	FLPRIME	FLDPRIME
0	-7.40258700E-09	.9839104451743	1.21162372E-02
1	.9891248875697	.9947232826917	7.65819069E-03
2	1.986430038235	.9992929571801	1.61321567E-03
3	2.986158517513	.999968760954	9.81590814E-05
4	3.986149003211	.999999238523	1.44328046E-06
5	4.986148509561	.9999995878902	4.04860163E-09

Table 5.4 (Continued)

**Table 6.1 Comparison Between Wall Shear Stress
for Large Blowing Parameter and Wall
Shear Stress for Single Fluid**

<u>β</u>	<u>$f_g(0)$</u>	<u>$f_g''(0)$</u>	
		<u>Program</u>	<u>Nickel [5]</u>
0	-1	0.0628	0
0.2	-1	0.2791	0.25
0.4	-1	0.4308	0.40
0.6	-1	0.5590	0.53
0.8	-1	0.6729	0.66
1.0	-1	0.7767	0.76
0.2	-1.25	0.1877	0.18
0.4	-1.25	0.3336	0.33
0.6	-1.25	0.4593	0.45
0.8	-1.25	0.5716	0.57

Table 6.2 Local Shear Stress Reduction (τ/τ_0)
as a Function of Wedge Angle and
Blowing Parameter for $R = 200$

f(0)	β					
	0	0.2	0.4	0.6	0.8	1.0
0.005	0.508	0.385	0.331	0.299	0.276	0.259
0.01	0.348	0.252	0.212	0.187	0.171	0.158
0.015	0.265	0.188	0.156	0.137	0.124	0.114
0.02	0.215	0.150	0.124	0.108	0.0972	0.0894
0.03	0.155	0.107	0.0874	0.0759	0.0681	0.0624
0.04	0.122	0.0833	0.0676	0.0585	0.0524	0.0479
0.05	0.100	0.0681	0.0551	0.0476	0.0426	0.0389
0.075	0.0691	0.0468	0.0377	0.0325	0.0291	0.0266
0.1	0.0526	0.0355	0.0287	0.0247	0.0221	0.0202
0.15	0.0353	0.0239	0.0193	0.0167	0.0150	0.0138
0.2	0.0262	0.0179	0.0145	0.0127	0.0115	0.0106
0.35	0.0138	0.00978	0.00826	0.00744	0.00692	0.00656
0.5	0.00827	0.00634	0.00567	0.00534	0.00515	0.00502
0.75	0.00337	0.00351	0.00363	0.00372	0.00379	0.00386
1.0	0.000720	0.00212	0.00261	0.00289	0.00309	0.00324

LIST OF REFERENCES

1. Pretsch, J., "Grenzen der Grenzschicht beeinflussung Zeitschrift der Angewandte Mathematik und Mechanik, Band 24, NR 5 und 6, pp. 264-267.
2. Ministry of Supply, Aeronautical Research Council (UK), Reports and Memoranda, R&M No. 2619, The Asymptotic Theory of Boundary-layer Flow with Suction, by E. J. Watson, pp. 1-45, September 1947.
3. Cess, R. D., and Sparrow, E. M., "Film Boiling in a Forced-Convection Boundary-Layer Flow," Journal of Heat Transfer, pp. 370-376, August 1961.
4. Ministry of Supply, Aeronautical Research Council (UK), Technical Report CP No. 157, Tabulation of the Blasius Function with Blowing and Suction, by Emmons, H. W., and Leigh, D. C., 1954.
5. Nickel, K., "Eine einfache Abschätzung für Grenzschichten," Ingenieur-Archiv, XXXI Band, Zweites Heft, pp. 85-100, 1962.
6. Cess, R. D., and Sparrow, E. M., "Subcooled Forced-Convection Film Boiling on a Flat Plate," Journal of Heat Transfer, pp. 377-379, August 1961.
7. Sparrow, E. M., Jonsson, V. K., and Eckert, E. R. G., "A Two-Phase Boundary Layer and Its Drag-Reduction Characteristics," Journal of Applied Mechanics, pp. 408-414, June 1962.
8. Eichenberger, H. P., and Offutt, J. D., About Gas Film Drag Reduction, paper presented at the Winter Annual Meeting of the ASME, New York, New York, 26 November - 1 December 1961.
9. Bradfield, W. S., Barkdoll, R. O., and Byrne, J. T., "Some Effects of Boiling a Hydrodynamic Drag," International Journal of Heat Mass Transfer, Vol. 5, pp. 615-622, 1962.
10. Lang, T. J., Torpedo Body Form and Gas Layer Control, U.S. Patent 3,205,846, 14 September 1965.

11. van Driest, E. R., "Problems of High Speed Hydrodynamics," Journal of Engineering for Industry, pp. 1-12, February 1969.
12. Schlichting, H., Boundary-Layer Theory, 7th edition, pp. 153-156, McGraw-Hill Book Company, 1979.
13. W. R. Church Computer Center, U.S. Naval Postgraduate School, Interactive Ordinary Differential Equation Package (IODE), by Hilleary, R. R., January 1978.
14. Sanders, J. V., Naval Postgraduate School, private communication, January - May 1982.

INITIAL DISTRIBUTION LIST

	<u>No. Copies</u>
1. Defense Technical Information Center Cameron Station Alexandria, Virginia 22314	2
2. Library, Code 0142 Naval Postgraduate School Monterey, California 93940	2
3. Department Chairman, Code 61 Department of Physics Naval Postgraduate School Monterey, California 93940	1
4. Associate Professor J. V. Sanders, Code 61Sd Department of Physics Naval Postgraduate School Monterey, California 93940	5
5. F. J. Jouailllec, Code 61Jl Department of Physics Naval Postgraduate School Monterey, California 93940	2
6. Inspecteur Onderwijs Zeemacht Ministry of Defense (Navy) Kon. Marialaan 17 Den Haag The Netherlands	2
7. Vlagofficier belast met de officiers vorming Koninklijk Instituut voor de Marine Het Nieuwe Diep 5 Den Helder The Netherlands	2
8. D. van Dord p/a Eekmolenweg 14 Wageningen The Netherlands	2

9. B. S. Papadales Jr.
Tactical Technology Office
Defense Advanced Research Projects Agency
1400 Wilson Boulevard
Arlington, Virginia 22209

1